

# Damage resistance and R-curve behavior of multilayer $\text{Al}_2\text{O}_3/\text{SiC}$ ceramics

Jihong She \*, Takahiro Inoue, Kazuo Ueno

*Department of Energy Conversion, Osaka National Research Institute, Midorigaoka 1-8-31, Ikeda, Osaka 563-8577, Japan*

Received 1 September 1999; received in revised form 14 September 1999; accepted 12 January 2000

## Abstract

Damage resistance and R-curve behavior of multilayer  $\text{Al}_2\text{O}_3/\text{SiC}$  ceramics were evaluated in bending by the indentation-strength and the single-edge-notched-beam methods. Due to the crack deflection at the  $\text{Al}_2\text{O}_3/\text{SiC}$  interfaces, a plateau indentation strength response was achieved, suggesting an exceptional resistance to contact-induced damage. Moreover, fracture toughness was observed to increase from 8.0 to 15.5  $\text{MPa m}^{1/2}$  with increasing notch depth from 0.5 to 2.0 mm, indicative of a strong R-curve behavior. © 2000 Elsevier Science Ltd and Techna S.r.l. All rights reserved.

**Keywords:** B. Interfaces; C. Fracture; C. Mechanical properties; D.  $\text{Al}_2\text{O}_3$

## 1. Introduction

In recent years, there has been considerable interest in the mechanical behavior of a variety of multilayer ceramic composites. It has been shown that enhanced strength and toughness in combination with improved damage resistance can be achieved for three-layer ceramic laminates consisting either of two strong outer layers and a tough inner layer [1,2] or of two compressive outer layers and a tensile inner layer [3–7]. On the other hand, increased apparent toughness and fracture energy as well as a non-catastrophic fracture behavior have been demonstrated for multilayer ceramic laminates by introducing weak interfaces [8–11] or by inserting porous layers [12] between ceramic substrates. However, little work [12] has been performed on the flaw tolerance and fracture resistance behavior of these laminates.

More recently, we have successfully fabricated a multilayer  $\text{Al}_2\text{O}_3/\text{SiC}$  ceramic [13]. Due to the deflection of through-thickness cracks at the weak SiC interfaces, such a laminate fails gracefully, and its apparent toughness and fracture energy are up to 15.1  $\text{MPa m}^{1/2}$  and 3335  $\text{J/m}^2$ , respectively. In this work, the damage resistance and R-curve behavior are further investigated.

## 2. Experimental procedure

The fabrication process of multilayer  $\text{Al}_2\text{O}_3/\text{SiC}$  ceramics has been described elsewhere [13]. Briefly, sub-micrometer  $\alpha\text{-Al}_2\text{O}_3$  powders (0.22  $\mu\text{m}$ , TM-D, Taimei Chemicals Co., Ltd., Japan) were extrusion-molded into 0.35-mm-thick sheets, then coated with a 50 vol% SiC-containing slurry, and finally hot-pressed in a graphite die under a 25-MPa pressure at 1500°C for 1 h. The resultant layered structure is shown in Fig. 1. As can be seen, the  $\text{Al}_2\text{O}_3/\text{SiC}$  interfaces are smooth and well-defined. The thicknesses of the  $\text{Al}_2\text{O}_3$  and SiC layers were determined to be  $182.7 \pm 10.1$  and  $12.9 \pm 1.4$   $\mu\text{m}$ , respectively.

To evaluate the fracture behavior, the hot-pressed billets were machined into the rectangular bars of 3 mm (thickness)  $\times$  4 mm (width)  $\times$  40 mm (length), and indented at the center of one polished tensile surface with a Vickers diamond pyramid indenter under loads ranging from 3 to 500 N. All indentations were made in air, and the indenter contacted the specimen surface for 30 s before it was withdrawn to complete the load cycle. Care was taken to orient one set of the indentation cracks to be parallel to the longitudinal axis of the rectangular bars. After indentation, the specimens were tested in three-point bending with a loading span of 30 mm and a crosshead speed of 0.5 mm/min. Three tests were performed at each indentation load.

\* Corresponding author at present address: Institute of Materials, German Aerospace Center (DLR), 51147 Köln, Germany. Fax: +49-2203-696480.

E-mail address: jhshe@hotmail.com (J. She).

On the other hand, a straight notch was introduced at the center part of the test bars of 3 mm in width, 4 mm in height, and 40 mm in length. The notch width was about 0.1 mm, and the notch depth was varied between 0.5 and 2.5 mm. Four-point bending tests were conducted on the notched specimens using an inner span of 10 mm and an outer span of 30 mm at a loading rate of 0.1 mm/min. Three to four specimens were tested for each notch depth.

### 3. Results and discussion

Fig. 2 shows the load–displacement curves of the indented and notched specimens under bending tests. Evidently, the fracture behavior of the indented specimen is similar to that of the notched specimen. Upon initial loading, both specimens behave elastically until a crack initiates at the notch tip or from the indent. Such

a crack propagates through the  $\text{Al}_2\text{O}_3$  layer itself, but is arrested at the interface with the adjacent SiC layer. As shown in Fig. 3, crack deflection occurs along or at close proximity to the  $\text{Al}_2\text{O}_3/\text{SiC}$  interface. Further loading causes the formation of some new cracks in the next  $\text{Al}_2\text{O}_3$  layer. This process is repeated until all the  $\text{Al}_2\text{O}_3$  layers have cracked, resulting in a step-like load–displacement response.

From the maximum load,  $P_i$ , in the load–displacement curve of the indented specimen, the indentation strength,  $\sigma_i$ , was calculated according to

$$\sigma_i = \frac{3P_i L}{2bt^2} \quad (1)$$

where  $L$  is the supporting span of the three-point bending fixture,  $b$  the specimen width, and  $t$  the specimen thickness. Fig. 4 shows the strengths of the specimens after indentation at different loads. Clearly, the indentation

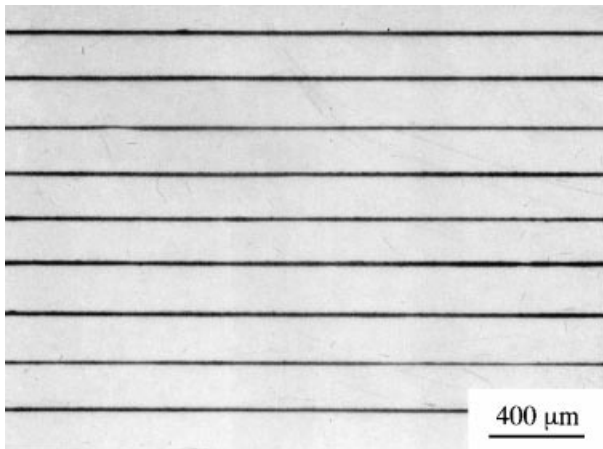


Fig. 1. Optical micrograph of the cross section of a representative specimen, showing a perfect layered structure.

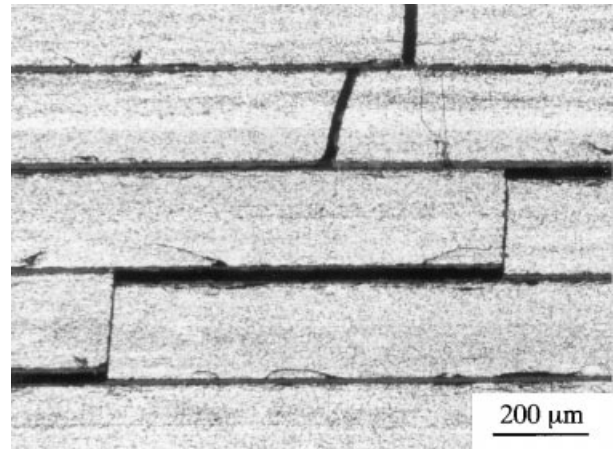


Fig. 3. Propagation of a major crack through the specimen. Note that crack deflection occurs along or at close proximity to the  $\text{Al}_2\text{O}_3/\text{SiC}$  interfaces.

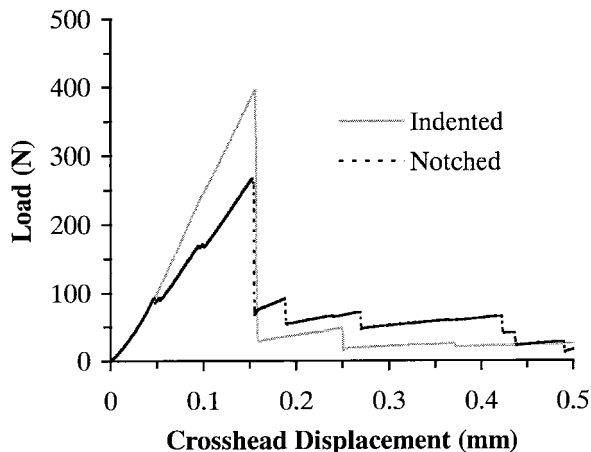


Fig. 2. Load–displacement curves of multilayer  $\text{Al}_2\text{O}_3/\text{SiC}$  ceramics with an indent (solid line) or a notch (dashed line) on the tensile surface.

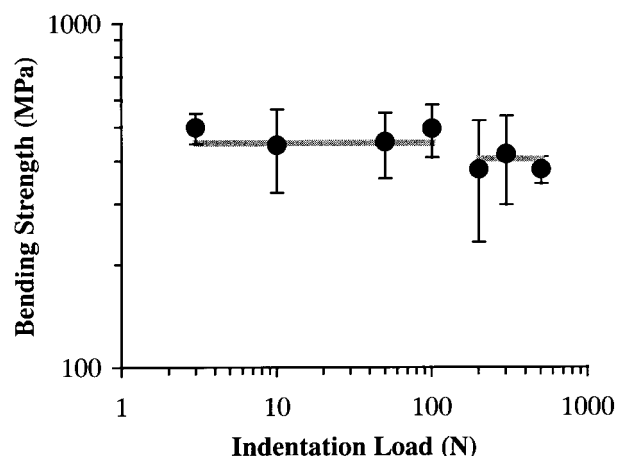


Fig. 4. Indentation strength response of multilayer  $\text{Al}_2\text{O}_3/\text{SiC}$  ceramics.

strengths are insensitive to the increases in the indentation load, indicative of excellent damage resistance. In fact, the indentation strength,  $\sigma_i$ , is related to the indentation crack depth,  $a$ , by

$$\sigma_i = \sigma_0 \left(1 - \frac{a}{t}\right)^2 \quad (2)$$

where  $\sigma_0$  is the fracture strength of the unindented specimens. Substituting the measured value of 497 MPa for  $\sigma_0$  and taking the indentation crack depth as the thickness of the individual  $\text{Al}_2\text{O}_3$  layers, one can obtain a calculated strength of 450 MPa. This suggests that as long as the indentation crack does not penetrate through the outer  $\text{Al}_2\text{O}_3$ -layer thickness, the indented specimen may retain its strength at a value of about 450 MPa. Based on the experiments of Lawn and co-workers [14,15], the indentation crack depth,  $a$ , can be estimated from

$$a = \left[ 0.016 \left( \frac{E}{H} \right)^{1/2} \cdot \frac{P}{K_{IC}} \right]^{2/3} \quad (3)$$

where  $E$  is the Young's modulus,  $H$  is the Vickers hardness,  $P$  is the indentation load, and  $K_{IC}$  is the fracture toughness. Using the experimental values of  $E = 343.2$  GPa,  $H = 16.1$  GPa, and  $K_{IC} = 5.32$  MPa  $\text{m}^{1/2}$ , the indentation crack depths at different loads were calculated and are listed in Table 1. When the indentation load is below 200 N, the estimated indentation-crack depth is smaller than the  $\text{Al}_2\text{O}_3$ -layer thickness of 182.7  $\mu\text{m}$ , indicating that the indentation crack is completely contained within the outer  $\text{Al}_2\text{O}_3$  layer. In this case, the indentation strengths should be kept at  $\sim 450$  MPa. As can be seen in Fig. 4, this strength value is in good agreement with the experimental data. When the indentation load is between 200 and 500 N, the indentation-induced crack may penetrate through the surface layer and into the second  $\text{Al}_2\text{O}_3$  layer. Due to the deflection of such a through-thickness crack along the interface with the second SiC layer, however, it is possible for the indented specimens to retain a fracture strength of  $\sim 405$

MPa. Again, this predicted value from Eq. (2) is consistent with the measured strengths of 376.5, 417.3 and 376.7 MPa for an indentation load of 200, 300 and 500 N, respectively. These results have clearly shown that multilayer  $\text{Al}_2\text{O}_3/\text{SiC}$  ceramics can retain a significant fraction of their strength even under contact damage conditions. This should allow them to exhibit superior resistance to impact- or abrasion-induced damage in service.

To evaluate the R-curve behavior, the fracture resistance,  $K_r$ , was computed from the results of the indentation strength measurements using the following equation [16]

$$K_r = 0.59 \left( \frac{E}{H} \right)^{1/8} (\sigma_i \cdot P^{1/3})^{3/4} \quad (4)$$

where  $\sigma_i$  is the fracture strength of the indented specimens at a load  $P$ . The computed fracture resistance is illustrated in Fig. 5 as a function of the estimated indentation-crack depth from Eq. (3). It can be seen in Fig. 5 that the fracture resistance increases with increasing indentation-crack depth, suggesting a strong R-curve effect of multilayer  $\text{Al}_2\text{O}_3/\text{SiC}$  ceramics.

Also, the rising R-curve behavior was observed in the fracture toughness measurements using the SENB (single-edge notched beam) method. Fig. 6 presents the measured  $K_{IC}$  values at different notch depths, in which the  $K_{IC}$  was calculated from the load maximum in the load–displacement curve of a notched specimen. As can be seen in Fig. 6, the measured fracture toughness increases from 8.0 to 15.5 MPa  $\text{m}^{1/2}$  as the notch depth increases from 0.5 to 2.0 mm.

On the other hand, the load–displacement curves of notched specimens were observed to be essentially the same, except for the decreased peak load with increasing notch depth. By assuming that the net section stress in

Table 1  
Estimated indentation-crack depths at different loads for multilayer  $\text{Al}_2\text{O}_3/\text{SiC}$  ceramics

Indentation load (N)	Crack depth ( $\mu\text{m}$ )
3	12.0
10	26.8
50	78.4
100	124.5
200	197.6
300	258.9
500	363.9

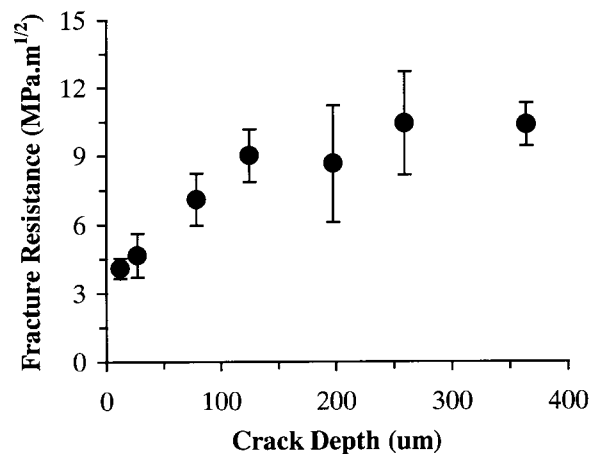


Fig. 5. Dependence of fracture resistance on crack depth for multilayer  $\text{Al}_2\text{O}_3/\text{SiC}$  ceramics.

the plane of the notch is constant, the nominal stress,  $\sigma_n$ , can be calculated from [17]

$$\sigma_n = \sigma_o \left(1 - \frac{a_o}{h}\right)^2 \quad (5)$$

where  $\alpha_o$  is the notch depth, and  $h$  is the specimen height. Fig. 7 shows the variation of nominal stress with normalized notch depth,  $a_o/h$ . For comparison, the measured nominal stresses at different notch depths are also shown in Fig. 7. Obviously, the calculated curve coincides well with the experimental data. This result indicates that the only effect of the notch is to reduce the net cross section of the beam. Due to the crack deflection at the  $\text{Al}_2\text{O}_3/\text{SiC}$  interfaces, the stress concentration associated with the notch may be effectively eliminated, resulting in the observed notch-insensitive behavior.

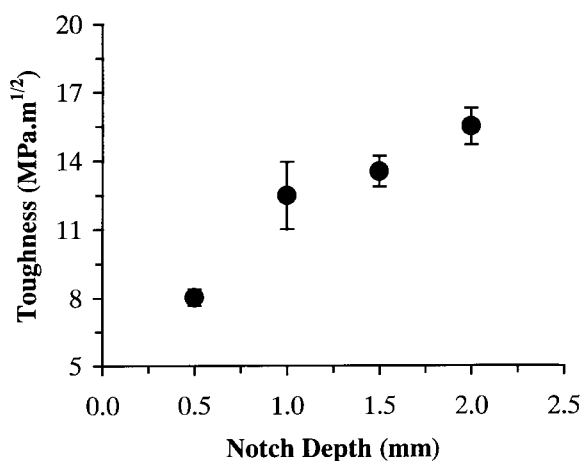


Fig. 6. Fracture toughness as a function of notch depth for multilayer  $\text{Al}_2\text{O}_3/\text{SiC}$  ceramics.

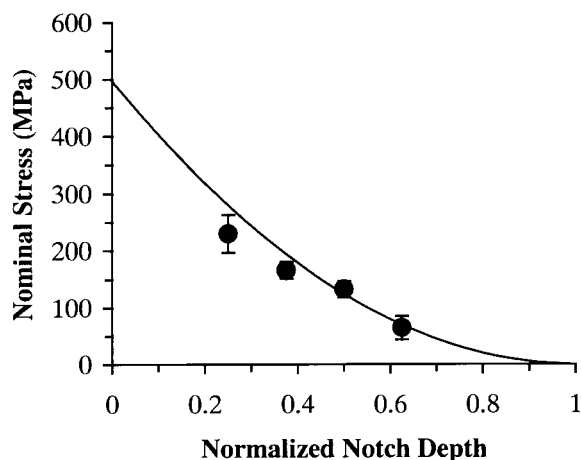


Fig. 7. Effect of the initial notch depth on the maximum nominal stress under 4-point bending tests. The solid line is calculated from Eq. (5).

## 4. Conclusions

Multilayer ceramic composites may exhibit some unique mechanical properties. In this work, the damage resistance and R-curve behavior of multilayer  $\text{Al}_2\text{O}_3/\text{SiC}$  ceramics were investigated using the indentation-strength and the single-edge-notched-beam methods. Due to the deflection of the transverse cracks along the  $\text{Al}_2\text{O}_3/\text{SiC}$  interfaces, the indentation strengths were observed to be insensitive to the increases in the indentation load, indicative of excellent damage resistance. Furthermore, a rising R-curve behavior was demonstrated from the results of the indentation-strength and the fracture-toughness measurements.

## Acknowledgements

Jihong She would like to thank the Agency of Industrial Science and Technology (AIST), Ministry of International Trade and Industry (MITI) for granting him an AIST Research Fellowship at Osaka National Research Institute, Japan.

## References

- [1] C.J. Russo, M.P. Harmer, H.M. Chan, G.A. Miller, Design of a laminated ceramic composite for improved strength and toughness, *J. Am. Ceram. Soc.* 75 (1992) 3396–3400.
- [2] B.J. Choi, K.H. Koh, H.E. Kim, Mechanical properties of  $\text{Si}_3\text{N}_4$ - $\text{SiC}$  three-layer composite materials, *J. Am. Ceram. Soc.* 81 (1998) 2725–2728.
- [3] J.H. She, S. Scheppokat, R. Janssen, N. Claussen, Reaction-bonded three-layer alumina-based composites with improved damage resistance, *J. Am. Ceram. Soc.* 81 (1998) 1374–1376.
- [4] O. Sbaizero, E. Lucchini, Influence of residual stresses on the mechanical properties of a layered ceramic composites, *J. Eur. Ceram. Soc.* 16 (1996) 813–818.
- [5] R. Sathyamoorthy, A.V. Virkar, R.A. Cutler, Damage-resistant  $\text{SiC}$ - $\text{AlN}$  layered composites with surface compressive stresses, *J. Am. Ceram. Soc.* 75 (1992) 1136–1141.
- [6] R.A. Cutler, J.D. Bright, A.V. Virkar, D.K. Shetty, Strength improvement in transformation toughened alumina by selective phase transformation, *J. Am. Ceram. Soc.* 70 (1987) 714–718.
- [7] J.J. Hansen, R.A. Cutler, D.K. Shetty, A.V. Virkar, Indentation fracture response and damage resistance of  $\text{Al}_2\text{O}_3$ - $\text{ZrO}_2$  composites strengthened by transformation-induced residual stresses, *J. Am. Ceram. Soc.* 71 (1988) C501–C505.
- [8] W.J. Clegg, The fabrication and failure of laminar ceramic composites, *Acta Metall. Mater.* 40 (1992) 3085–3093.
- [9] W.J. Clegg, K. Kendall, N.M. Alford, T.W. Button, J.D. Birchall, A simple way to make tough ceramics, *Nature* 347 (1990) 455–457.
- [10] H. Liu, S.M. Hsu, Fracture behavior of multilayer silicon nitride/boron nitride ceramics, *J. Am. Ceram. Soc.* 79 (1996) 2452–2457.
- [11] D. Kovar, M.D. Thouless, J.W. Halloran, Crack deflection and propagation in layered silicon nitride/boron nitride ceramics, *J. Am. Ceram. Soc.* 81 (1998) 1004–1012.
- [12] T. Ohji, Y. Shigegaki, T. Miyajima, S. Kanzaki, Fracture resistance behavior of multilayered silicon nitride, *J. Am. Ceram. Soc.* 80 (1997) 991–994.

- [13] J.H. She, T. Inoue, K. Ueno, Multilayer  $\text{Al}_2\text{O}_3/\text{SiC}$  ceramics with improved mechanical behavior, *J. Eur. Ceram. Soc.*, 20 (2000) 1771–1775.
- [14] B.R. Lawn, A.G. Evans, D.B. Marshall, Elastic/plastic indentation damage in ceramics: the median/radial crack system, *J. Am. Ceram. Soc.* 63 (1980) 574–581.
- [15] G.R. Anstis, P. Chantikul, B.R. Lawn, D.B. Marshall, A critical evaluation of indentation techniques for measuring fracture toughness: I. Direct crack measurements, *J. Am. Ceram. Soc.* 64 (1981) 533–538.
- [16] P. Chantikul, G.R. Anstis, B.R. Lawn, D.B. Marshall, A critical evaluation of indentation techniques for measuring fracture toughness: I. Strength method, *J. Am. Ceram. Soc.* 64 (1981) 539–543.
- [17] C.A. Folsom, F.W. Zok, F.F. Lange, D.B. Marshall, Mechanical behavior of a laminar ceramic/fiber-reinforced epoxy composite, *J. Am. Ceram. Soc.* 75 (1992) 2969–2975.